JACS Au
AN OPEN ACCESS JOURNAL OF THE AMERICAN CHEMICAL SOCIETY

pubs.acs.org/jacsau
Article

Engineering Gene-Specific DNAzymes for Accessible and Multiplexed Nucleic Acid Testing

Lu Gao,[⊥] Ke Yi,[⊥] Yun Tan, Chen Guo, Danxi Zheng, Chenlan Shen, and Feng Li*

Cite This: JACS Au 2024, 4, 1664−1672
Read Online

ACCESS | Metrics & More | Article Recommendations | Supporting Information

ABSTRACT: The accurate and timely detection of disease biomarkers at the point-of-care is essential to ensuring effective treatment and epidemiological surveillance. Here, we report the selection and engineering of RNA-cleaving DNAzymes that respond to specific genetic markers and amplify detection signals. Because the target-specific activation of gene-specific DNAzymes (gDz) is like the trans-cleavage activity of clustered regularly interspaced short palindromic repeats (CRISPR) CRISPR-associated (Cas) machinery, we further developed a CRISPR-like assay using RNA-cleaving DNAzyme coupled with isothermal sequence and signal amplification (CLARISSA) for nucleic acid detection in clinical samples. Building on the high sequence specificity and orthogonality of gDzs, CLARISSA is highly versatile and expandable for multiplex testing. Upon integration with an isothermal recombinase polymerase amplification, CLARISSA enabled the detection of human papillomavirus (HPV) 16 in 189 cervical samples collected from cervical cancer screening participants (n = 189) with 100% sensitivity and 97.4% specificity, respectively. A multiplexed CLARISSA further allowed the simultaneous analyses of HPV16 and HPV18 in 46 cervical samples, which returned clinical sensitivity of 96.3% for HPV16 and 83.3% for HPV18, respectively. No false positives were found throughout our tests. Besides the fluorescence readout using fluorogenic reporter probes, CLARISSA is also demonstrated to be fully compatible with a visual lateral flow readout. Because of the high sensitivity, accessibility, and multiplexity, we believe CLARISSA is an ideal CRISPR-Dx alternative for clinical diagnosis in field-based and point-of-care applications.

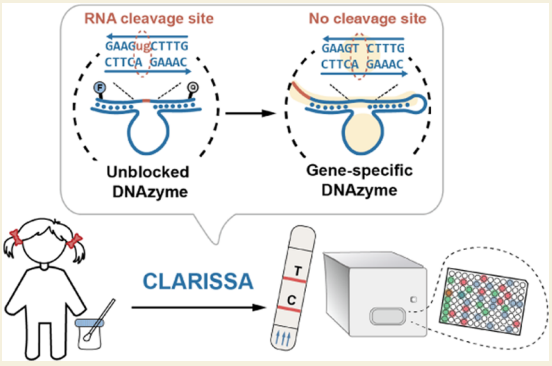

KEYWORDS: *DNAzyme, molecular diagnosis, nucleic acid testing, point-of-care, isothermal nucleic acid amplification*

INTRODUCTION

The accurate and timely detection of disease biomarkers is essential to ensure the effective treatment and epidemiological surveillance.[1−4] Nucleic acid testing (NAT) capable of detecting trace amount of disease-related DNA or RNA via nucleic acid amplification has become the gold standard for various infectious and somatic diseases.[3,5−7] However, standard NATs relying on polymerase chain reaction (PCR) require costly equipment and trained personnel and thus can only be used in centralized facilities.[8] The ongoing need to enable accurate testing at home and at the point-of-care (POC) demands the field-deployable NATs with high assay performance but low infrastructural requirements.[9−12] Toward this goal, clustered regularly interspaced short palindromic repeats (CRISPR) and CRISPR-associated (Cas) systems are currently revolutionizing NATs by offering exceptional sensitivity, specificity, and accessibility.[13−20] A parrel effort was also made to engineer deoxyribozymes (DNAzymes) into CRISPR-like tools for gene editing and disease diagnostics because DNAzymes also possess RNA/DNA-cleaving activities but with no need for protein components.[21−24] However, existing DNAzymes do not possess sequence selectivity to nucleic acid targets. To address this challenge, Mokany et al. introduced a multicomponent DNAzyme (MNAzyme) design that allowed the detection of any nucleic acid target by splitting the catalytic core of a DNAzyme into two parts, each of which was extended with a complementary domain to a given target nucleic acid.[25] Chan and colleagues further developed genetic tests deployable for POCT by integrating MNAzymes with nanoparticles.[26,27] Nevertheless, the splitting of the catalytic core sequence would inevitably lead to reduced enzymatic activity, and significant effort has to be made to optimize the splitting site to minimize this effect. To compensate for the reduction of activity, Chaput and colleagues introduced chemical modifications to MNAzymes, which successfully enhanced overall assay performances. A further integration with recombinase polymerase amplification (RPA), sensitive

Received: March 13, 2024
Revised: April 1, 2024
Accepted: April 2, 2024
Published: April 9, 2024

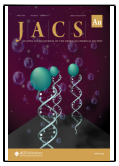

https://doi.org/10.1021/jacsau.4c00232
JACS Au 2024, 4, 1664−1672

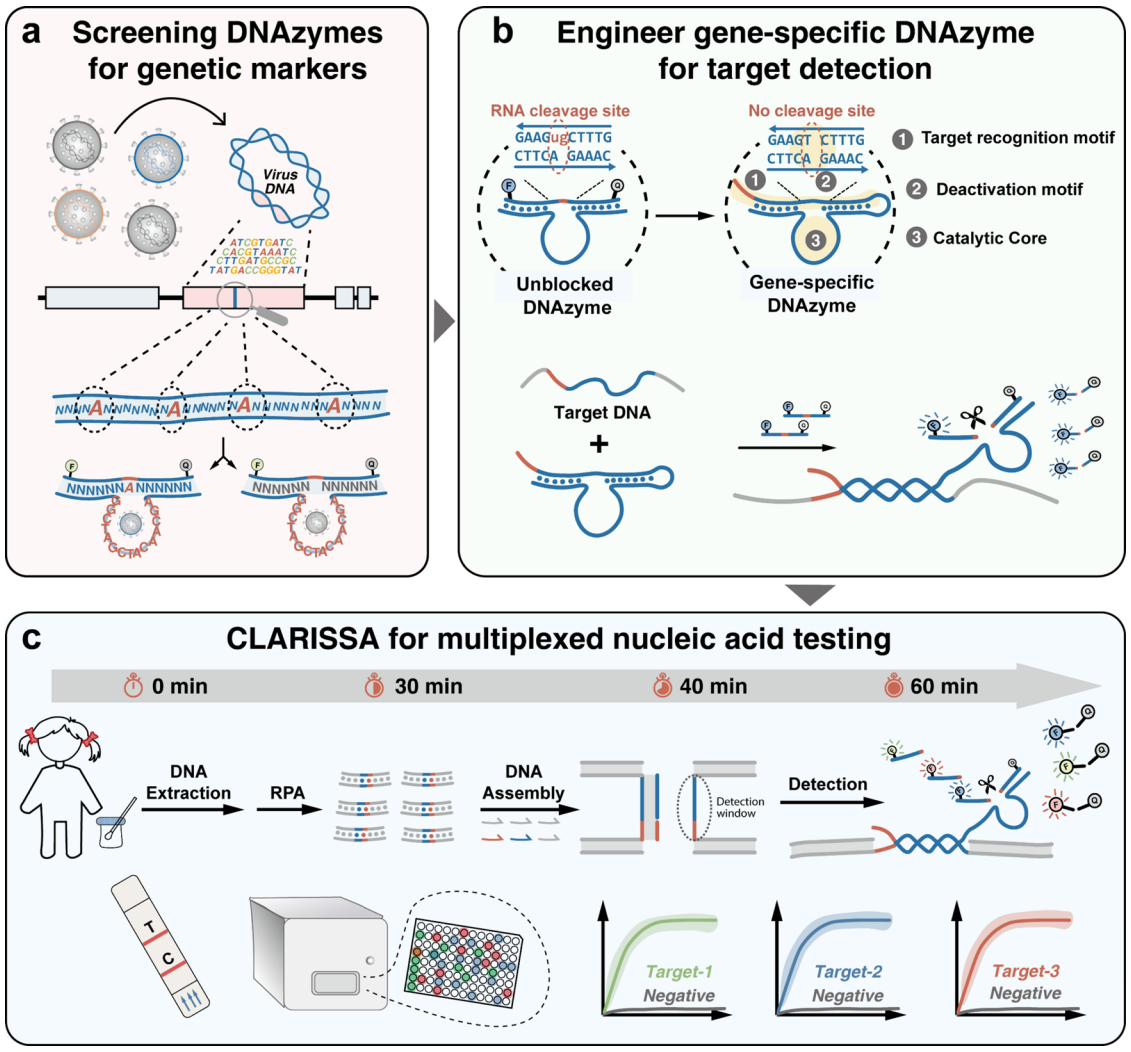

Figure 1. Overview of CLARISSA. (a) Schematic illustration of screening DNAzymes for genetic markers. (b) Engineering gene-specific DNAzymes for target detection. (c) The workflow for clinical diagnosis is using multiplexed CLARISSA.

detection of severe acute respiratory syndrome coronavirus 2 (SARS-CoV-2) and its mutants were achieved in clinical samples.[28−30] Although chemical modification could effectively rescue the split DNAzymes, it increases the upfront cost and accessibility of the test. An ideal engineering approach to achieve target-specific DNAzymes in a cost-effective manner should keep its integrity to ensure maximal enzymatic activity. Thus, driven, we report an alternative design principle for engineering gene-specific DNAzymes (gDz) by directly screening the arm sequences of an RNA-cleaving DNAzyme against a genetic marker of interest (Figure 1a). The selected gDz is then further engineered using a DNA motif to block the arm sequences (Figure 1b). A toehold motif is also engineered for gDz, so that it can be effectively activated in the presence of the target gene. By further integrating gDz with RPA through a DNA assembly strategy, we finally develop a CRISPR-Like Assay using RNA-cleaving DNAzyme coupled with Isothermal Sequence and Signal Amplification (CLARISSA), a NAT platform with attomolar sensitivity (Figure 1c). CLARISSA enabled the detection of human papillomavirus (HPV) 16 in 189 cervical samples collected from cervical cancer screening participants (n = 189) with a 100% sensitivity and 97.4% specificity, respectively. Because both target recognition and signal amplification are streamlined within a single-stranded DNA construct, our gDz offers enhanced design space over multicomponent designs for multiplexed NAT (Figure 1c). To demonstrate this potential, we further developed a multiplex CLARISSA that enabled the simultaneous analyses of HPV16, HPV18, and the human β-globin gene in 46 cervical samples, which returned a clinical sensitivity of 96.3% for HPV16 and 83.3% for HPV18, respectively.

RESULTS AND DISCUSSION

Screening DNAzymes for Genetic Markers

The design of gDzs begins by reproposing a 10−23 RNA-cleaving DNAzyme for specific genetic biomarkers.[31,32] As a proof-of-concept, we first designed a panel of Dzs for human β-globin by keeping the 15 nt catalytic core of 10−23 Dz but screening binding arm sequences against the genome sequence (Figure 2a). The arm lengths were designed to be 6−8 nt on each side with binding strengths ranging from −9.61 to −12.69 kcal/mol, so that each Dz offers both high catalytic efficiency and sequence specificity to the target gene. All sequences were examined using NUPACK software to avoid secondary structures and homodimers (Supporting Table 1). Using the same approach, we also designed Dzs targeting the L1 gene of human papillomavirus (HPV) strains 16 and 18. L1 genes were

https://doi.org/10.1021/jacsau.4c00232
JACS Au 2024, 4, 1664−1672

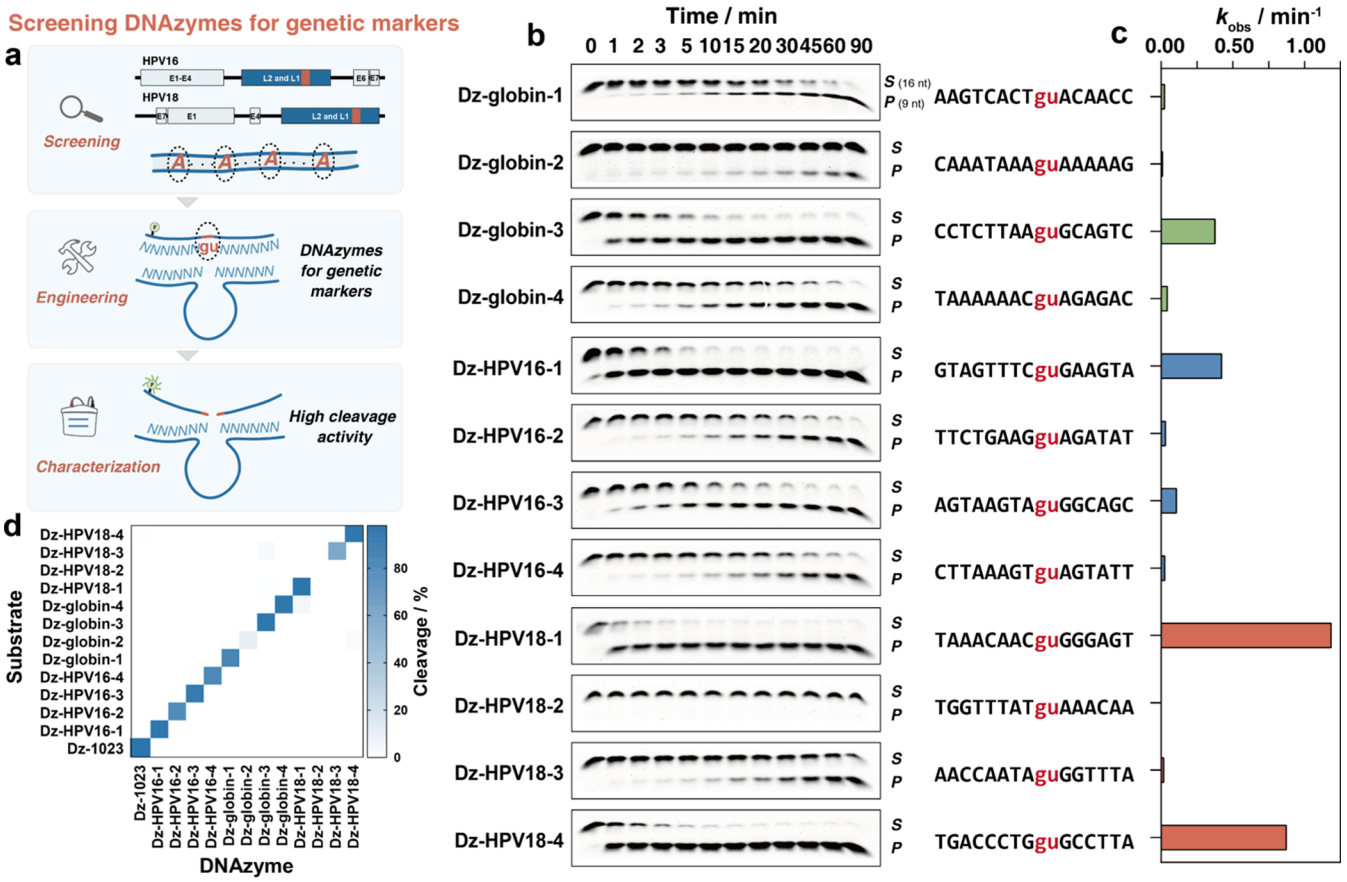

Figure 2. Screening and characterization of DNAzymes for genetic markers. (a) Schematic illustration of the workflow for screening Dzs for genetic markers. Gene-specific sequences containing an adenosine in the middle were searched against BLAST to ensure sequence selectivity, as well as NUPACK to ensure minimal secondary structures. These Dzs were then designed by integrating the catalytic core of 10−23 Dz with the gene-specific arm sequences. The catalytic activities were then characterized by using fluorescently labeled substrates and PAGE analyses. (b) Characterization of catalytic activities of Dzs was performed using PAGE analysis. (c) Presteady-state kinetic analysis was used to determine observed rate constants of Dzs. (d) Heat map to illustrate the orthogonality of Dzs to varying substrate sequences.

chosen as targets of interest because of their high sequence conserveness and low similarity to other subtypes.[33,34]

To characterize the catalytic efficiency for these screened Dzs, fluorescently labeled substrates were designed and analyzed using polyacrylamide gel electrophoresis (PAGE) at varying time spots and under different conditions (Figure 2b and Supporting Figure 1). Results in Figure 2b revealed highly diverse catalytic efficiencies in a panel of 12 selected Dzs. These Dzs, such as Dz-HPV18−2 displayed low or nearly no cleavage activity, whereas Dz-HPV18−1 showed the highest catalytic activity with an apparent rate constant k_{obs} = 1.186 min^{-1} (Figure 2c and Supporting Figure 2). To gain insight into the diversified enzymatic activities of the 12 selected gDzs, we plotted the observed rate constants against the formation energies of the gDz-substrate complexes, revealing that a minimal formation energy must be reached to ensure sufficient enzymatic activity (Supporting Figure 3). Under optimal conditions, we estimated that as little as 0.1 nM Dz could be detected using fluorogenic substrates as reporters (Supporting Figure 4). By subsequently mixing each selected Dzs with one of the 12 substrates, we also confirmed that the cleavage activities of all Dzs were highly orthogonal using PAGE analysis (Figure 2d and Supporting Figure 5) and fluorescence analysis, respectively (Supporting Figures 6 and 7), demonstrating the possibility to design multiplexed NATs by feeding gDzs with sequence-specific substrates as reporter probes.

Engineering Gene-Specific DNAzymes for the Detection of Genetic Markers

Having screened a panel of Dzs for genetic markers, we next engineered gDzs that can be activated by the target genes. To do so, a Dz with arm sequences screened against a subgenomic sequence was deactivated by blocking the arm sequences using a complementary DNA motif (Figure 3a). Because the complementary sequence did not contain the ribonucleotide, no cleavage could be made, and gDz was thus inactive in this construct. A toehold domain was also engineered as the complementary motif for effectively activating gDz upon target recognition. In the presence of the target gene, a strand displacement reaction was initiated through the toehold domain, which regenerated the Dz and unleashed its catalytic activity (Figure 3b and Supporting Table 2). By systematically optimizing all design parameters, we determined an optimal engineered gDz construct with an 8 nt toehold domain (Supporting Figure 8), a 23 bp complementary domain that was split into 8 and 15 bp by the catalytic core (Supporting Figure 9), and a 4 nt loop domain (Supporting Figure 10).

By measuring the initial rates of Dz-HPV18−1 and gDz-HPV18−1 at varying substrate concentrations, we found that the target-activated gDzs showed near identical cleavage activities with Dzs under the optimal sequence design (Figure 3c and Supporting Figures 11 and 12). More importantly, the catalytic efficiencies (k_{cat}/K_M) of gDzs were 0.6 × 10^6 M^{-1} s^{-1},

https://doi.org/10.1021/jacsau.4c00232
JACS Au 2024, 4, 1664−1672

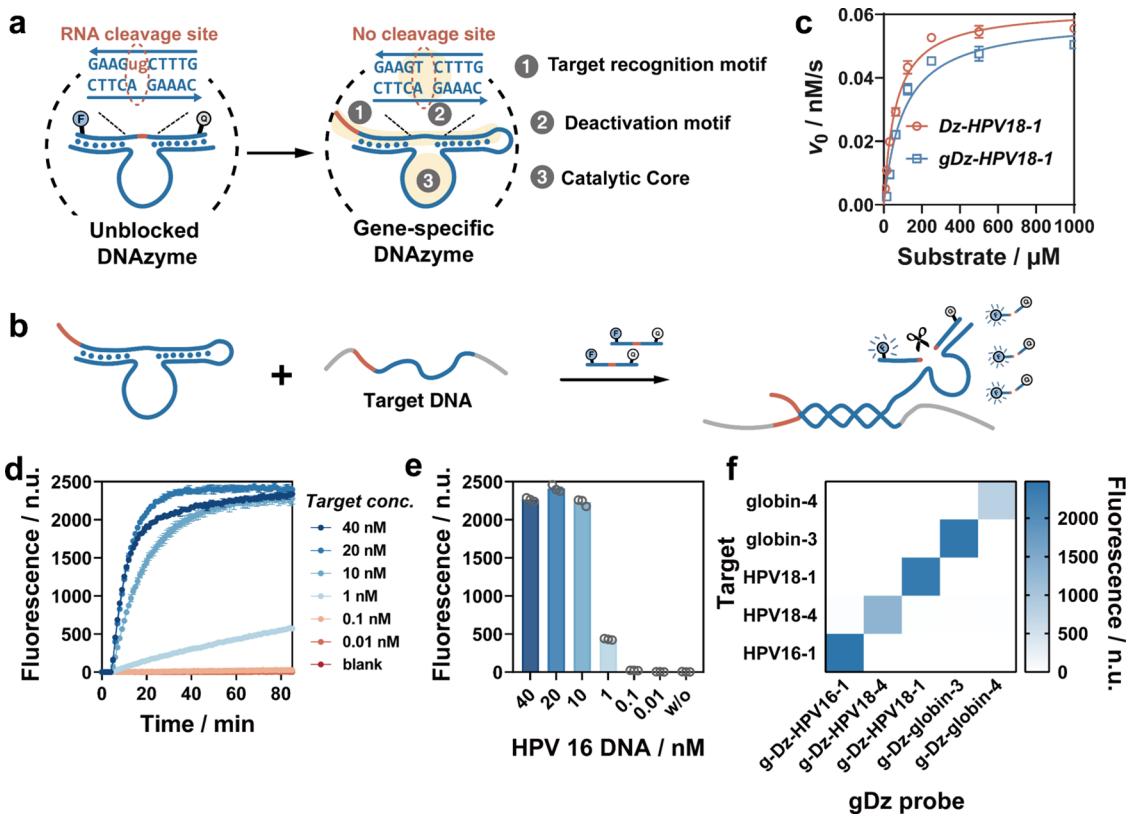

Figure 3. Engineering and characterization of gene-specific DNAzymes. (a) The design principle for engineering Dzs into gDzs involves deactivating the catalytic activity using an intramolecular complementary sequence that does not contain the ribonucleotide. (b) Schematic illustration of the activation of gDzs using a target DNA through toehold-mediated DNA strand displacement. (c) Michaelis−Menten analyses were of Dz-HPV18−1 and target-activated gDz-HPV18−1. Each error bar represents a standard deviation from triplicate analyses. (d) Kinetic curves for the detection of varying concentrations of HPV16 DNA were obtained using gDz-HPV16−1. (e) End point fluorescence at 60 min against the concentration of HPV-16 DNA. Technical triplicate was performed for each sample (n = 3). (f) Heat map to illustrate the orthogonality of gDzs to varying target genes.

which were in the same order of magnitude with some of the reported values of LbCas12a and LbuCas13a.[35−37] As low as 1 nM subgenomic sequence of HPV16 could effectively activate gDz-HPV16−1 and generate clearly distinguishable fluorescence signals (Figure 3d,e). Moreover, gDz is composed solely of an ssDNA, and thus demonstrated better stability than protein and RNA-based CRISPR systems against experimental conditions, such as freeze−thaw cycles and heating (Supporting Figures 13 and 14). We also examined the thermal stability of engineered gDzs using melting analysis (Supporting Figure 15). The high T_m values (>65 °C) of typical gDz designs suggest that gDzs were thermally stable at room temperature or 37 °C, which is critical to ensure low background signals for NAT. The activation of gDzs was also confirmed to be highly specific to the target gene, which is critical to establish gDzs for multiplex NATs (Figure 3f and Supporting Figures 16 and 17).

Integration of Gene-Specific DNAzyme with RPA

To enable NAT with gDzs, a critical step is to integrate gDz with RPA to develop CLARISSA.[38] In our study, we screened and optimized RPA primers (Supporting Table 3) for target genes of human β globin, HPV16, and HPV18 to generate amplicons capable of activating gDz-globin-3, gDz-HPV16−1, and gDz-HPV18−1, respectively (Supporting Figures 18−21). Because RPA produces double-stranded amplicons (ds-amplicons), it is critical to convert the ds-amplicon into a single-stranded amplicon (ss-amplicon). Moreover, the long ss-amplicon of RPA also tends to form secondary structures and homodimers, which may significantly reduce the hybridization efficiency with gDzs. To address these challenges, we introduce a panel of DNA helper strands that fold the ds-amplicon into two assemblies only exposing a short single-stranded detection window for gDz through a rapid heating and snap cooling step (Figure 4a and Supporting Figure 22 and Table 4).[39] To avoid background signals generated through the cross-reactions between gDz and DNA helpers, helper-2 was designed to contain only the complementary domain to the toehold, and helper-3 was only complementary to the branch migration domain of gDz. It is also critical to optimize the concentration of DNA helpers to minimize the direct strand displacement between helper-3 and gDz (Supporting Figure S23). To ensure optimal analytical performance, we also systematically optimized all reaction conditions (Supporting Figures 24 and 25). The kinetic curves in Figure 4b revealed that our assembly approach effectively integrated gDz-HPV16−1 with RPA and that as low as 1 aM genomic DNA could be clearly distinguished from the blank (Figure 4c). Besides HPV16, we also designed CLARISSA for the HPV 18 gene with single-digit attomolar sensitivity (Figure 4d and Supporting Figure 26).

Toward the goal of NAT in POC settings, we also engineered a field-deployable, visual lateral flow assay (LFA) readout for CLARISSA, which was achieved by replacing the fluorogenic reporter with a FAM-biotin dual-labeled reporter (Figure 4e). In the absence of the target gene, all anti-FAM-

https://doi.org/10.1021/jacsau.4c00232
JACS Au 2024, 4, 1664−1672

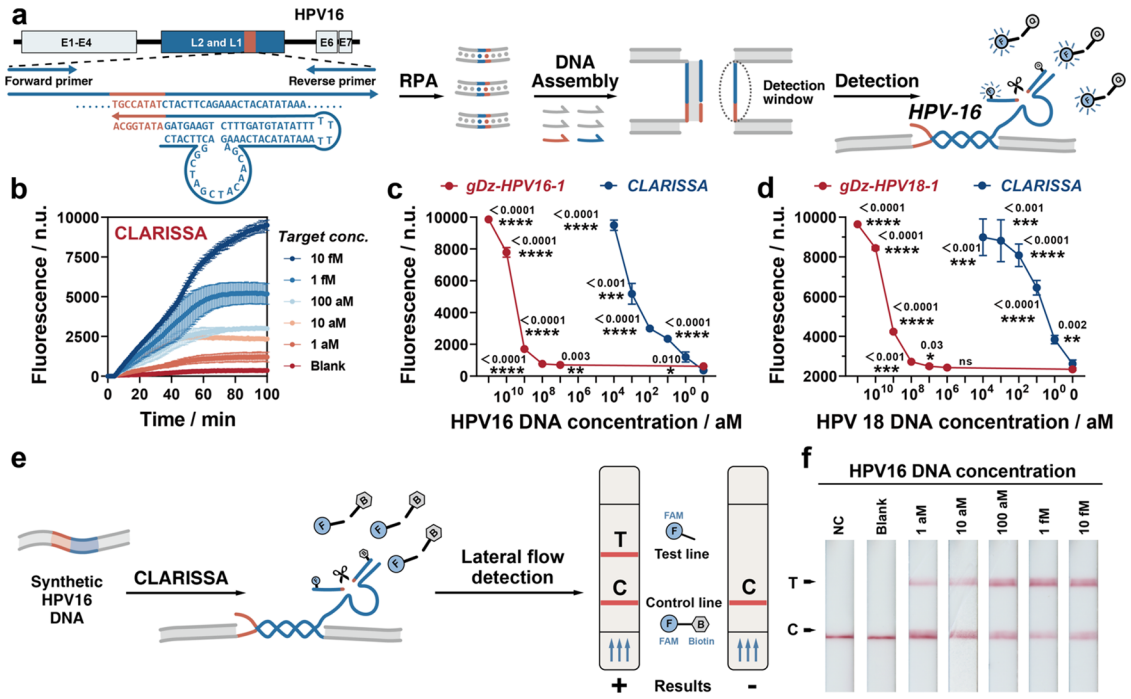

Figure 4. CLARISSA for the detection of HPV16 DNA. (a) Schematic illustration of the workflow of CLARISSA. (b) Kinetic curves were used for analyzing varying concentrations of HPV16 DNA using CLARISSA. (c, d) End point fluorescence at 100 min was plotted against varying concentrations of HPV16 (c) and HPV18 (d) DNA using both CLARISSA and gDz only. Each error bar represents one standard deviation from triplicate analyses. Unpaired *t-test* was used for all statistical analyses. (e) Design of reporter probes and lateral flow strips was done for the visual readout of CLARISSA. (f) Visual detection of HPV16 DNA with concentrations from 1 aM to 10 fM using CLARISSA coupled with LFA readout. NC stands for the negative control that contained only a FAM-biotin dual-labeled reporter probe.

labeled gold nanoparticles (AuNPs) were captured at the control line (C line) by the reporter. Upon CLARISSA, the reporter was cleaved, and AuNPs were further migrated and captured at the test line (T-line). As shown in Figure 4f, CLARISAA coupled with LFA allowed the visual detection of HPV16 with a LOD at 10 aM, though a slight background was observed in the absence of the target (Supporting Figure 27).

Clinical Validation of CLARISSA

Next, we tested the feasibility of CLARISSA for detecting HPV16 in clinical cervical samples. We began by extracting DNA from 189 cervical samples collected from cervical cancer screening at the West China Hospital of Sichuan University using a commercial column extraction kit and then validated CLARISSA for the detection of HPV16 infection (Supporting Table 5). All samples were clinically tested using standard PCR-reverse dot blot HPV genotyping test, which confirmed 38 HPV-16 positives and 151 negatives. All 189 cervical samples were then tested using CLARISSA, which returned significant differences between the positive and negative cohorts ($p < 0.0001$, $n = 189$) (Figure 5c). The optimal cutoff value for the CLARISSA-based HPV16 test was then established using receiver operating characteristic (ROC) curve analysis (Figure 5d). Upon benchmarking against the standard clinical PCR-Reverse Dot Blot test, we determined that the clinical sensitivity and specificity of CLARISSA were 97.4 and 100%, respectively (Figure 5e), demonstrating the high clinical potential of CLARISSA. We also validated CLARISSA with LFA readout for visual detection of HPV16 in clinical cervical samples ($n = 30$) (Figure 5f and Supporting Figure 28). CLARISSA coupled with LFA allowed the identification of 14 out of 15 HPV16 positives using the naked eye (Figure 5g and Supporting Figure 29d). All 15 negative samples were also correctly identified using CLARISSA, confirming the high sensitivity and specificity of the visual readout (Supporting Figure 29f). Notably, sample 29 clinically tested to be positive was found to be negative by two independent CLARISSA tests with fluorescence and visual readout, respectively. We speculated that this false negative result was caused by the sample treatment step rather than the CLARISSA.

Multiplexed NAT Using CLARISSA

Because each gDz can cleave its corresponding reporter with high orthogonality, CLARISSA is an ideal platform for multiplexed NAT. The World Health Organization (WHO) recommends DNA testing as a first-choice screening method for cervical cancer prevention and the two high-risk HPV strains (16 and 18) cause more than 70% of cervical cancers.[40,41] Therefore, we demonstrate the multiplexity of CLARISSA by simultaneously detecting high-risk HPV subtypes 16 and 18 in clinical cervical samples. To do so, gDz-HPV16−1 with ROX-labeled reporter probes and gDz-HPV18−1 with Cy3-labeled reporter probes were mixed as multiplexed sensing components. gDz-globin-3 with FAM-labeled reporters was also included to detect the human β-globin gene as a control of sampling and assay quality, which is a common practice in commercial PCR kits for HPV testing. All three gDzs and reporter probes were found to be highly specific and orthogonal in the multiplex assay format with no signal leakage (Supporting Figure 30). We also designed and optimized primers and helper DNA strands for the 3-plex RPA, so that all three genetic markers were effectively amplified and assembled simultaneously (Supporting Figures 31 and 32). The 3-plex CLARISSA was also confirmed to be highly specific to each of the target genes (Supporting Figure 33). Because

https://doi.org/10.1021/jacsau.4c00232
JACS Au 2024, 4, 1664−1672

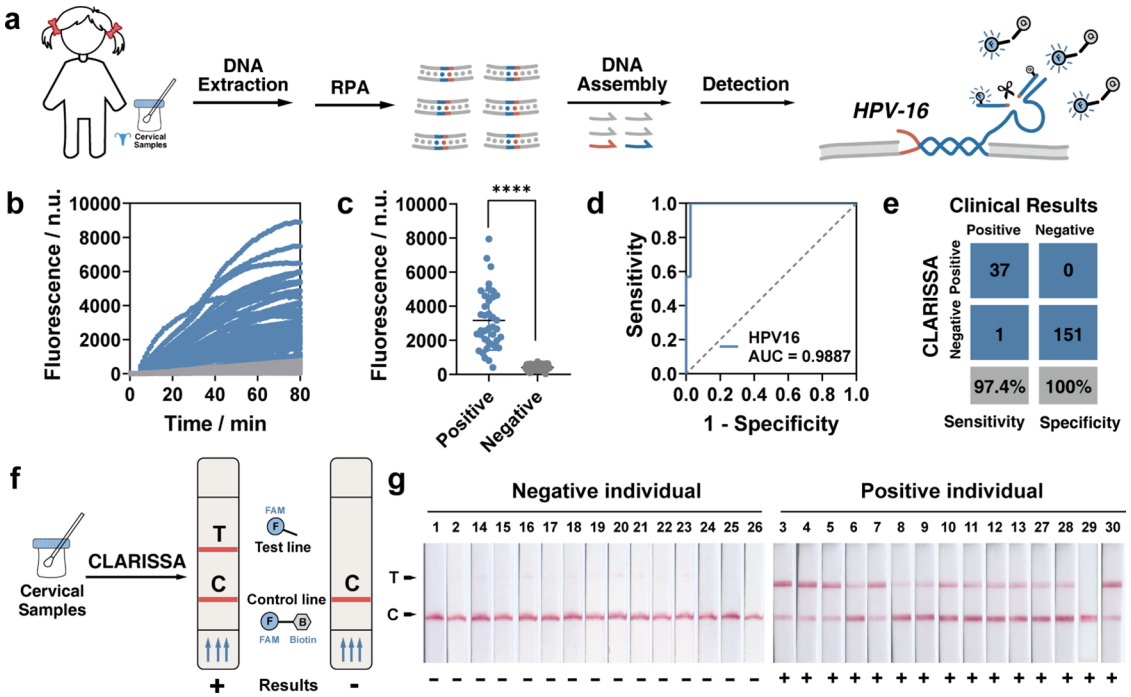

Figure 5. Clinical validation of CLARISSA. (a) The workflow for detecting HPV infection in clinical cervical samples was performed using CLARISSA. (b) Kinetic curves of CLARISS for analyzing HPV16 in 189 cervical samples collected from participating in cervical cancer screening. (c) CLARISSA test results of two clinical cohorts were obtained, including 38 positive samples and 151 negative samples. Unpaired two-tailed *t*-tests were used to evaluate statistical differences between the positive and negative cohorts. (d) ROC curve of CLARISSA for detecting HPV16 DNA in 189 human cervical samples (positive: n = 38, negative: n = 151). Optimal cutoff fluorescence values were selected through ROC analysis: 775 nuclei at 60 min for HPV16 (specificity = 100%; sensitivity = 97.4%). (e) Evaluation of the clinical sensitivity and specificity of CLARISSA by comparison to clinical screen tests using a confusion matrix (n = 151 for negative samples and n = 38 for positive samples). (f) Schematic illustration of the CLARISSA-based clinical tests using an LFA visual readout. g. Visual detection of 15 HPV16 positive clinical samples and 15 HPV16 negative samples using CLARISSA was coupled with LFA readout.

the primer concentrations were lower in the 3-plex RPA than those for singlet RPA to minimize cross-reactions, reduced amounts of RPA amplicons led to a slight decrease in the overall CLARISSA sensitivity. We then validated the 3-plex CLARISSA by analyzing 46 clinical cervical samples collected from patients undergone cervical cancer screening (Supporting Table 5). Kinetic curves in Figure 5b show that the human β-globin gene was detected in all 46 samples, suggesting that gDNA was successfully extracted and analyzed by CLARISSA in all cervical samples. Further kinetic analyses show that fluorescence signals at 60 min displayed optimal assay sensitivity for both HPV16 and HPV18 (Supporting Figure 34). Nevertheless, even fluorescence signals at 20 min were sufficient for detecting HPV16 and HPV18 DNA at 1 aM (Supporting Figure 35). Of the 46 clinical samples, the 3-plex CLARISSA identified 26 HPV16 positives (Figure 6c) and 5 HPV18 positives (Figure 6d) with significant differences found between the positive and negative cohorts (Figure 6e,f). Optimal cutoff values for both HPV16 and HPV18 within the 46 clinical cervical samples were then determined by using ROC curve analysis (Figure 6g). The test results of the 3-plex CLARISSA were then compared with the clinical test results using a confusion matrix (Figure 6h,i). The sensitivity and specificity of CLARISSA were determined to be 96.3% and 100% for HPV16 and 83.3 and 100% for HPV18, respectively. Altogether, within 189 samples tested using singlet or 3-plex CLARISSA tests, we only found two instances where CLARISSA were not in agreement with standard PCR-reverse dot blot HPV genotyping test. No false positives were found throughout our study.

CONCLUSIONS

To summarize, we have successfully introduced a novel design principle that enables DNAzymes for NAT. Our gDz design is achieved by directly screening arm sequences against genetic markers of interest. Therefore, the overall construct of gDz is a single-stranded DNA rather than a multicomponent design. The simple and straightforward design principle enables sequence-specific and orthogonal gDzs amenable for multiplex NAT. To further engineer gDz as NAT in clinical settings, we integrate gDz with RPA through a DNA assembly strategy, allowing the development of CLARISSA for highly sensitive and multiplexed NAT. The potential of CLARISSA for clinical uses was demonstrated by detecting gDNA of HPV16 and HPV18 in a total of 189 cervical samples collected from patients undergone HPV screening. Beyond high clinical consistency with standard HPV DNA-based screen tests, CLARISSA, like CRISPR-Dx, is an isothermal NAT technology with minimal equipment need. We further demonstrated that CLARISSA is fully adaptable with a visual LFA readout for tests in clinical settings. Therefore, CLARISSA is an ideal POCT capable of shifting HPV tests or other types of NATs from central diagnostic laboratories to resource-limited conditions. One current limitation of CLARISSA is the need for the heating and snap cooling protocol, which added the complexity of the test. In future studies, we aim to develop microfluidic chips and portable heating devices that are fully

https://doi.org/10.1021/jacsau.4c00232
JACS Au 2024, 4, 1664−1672

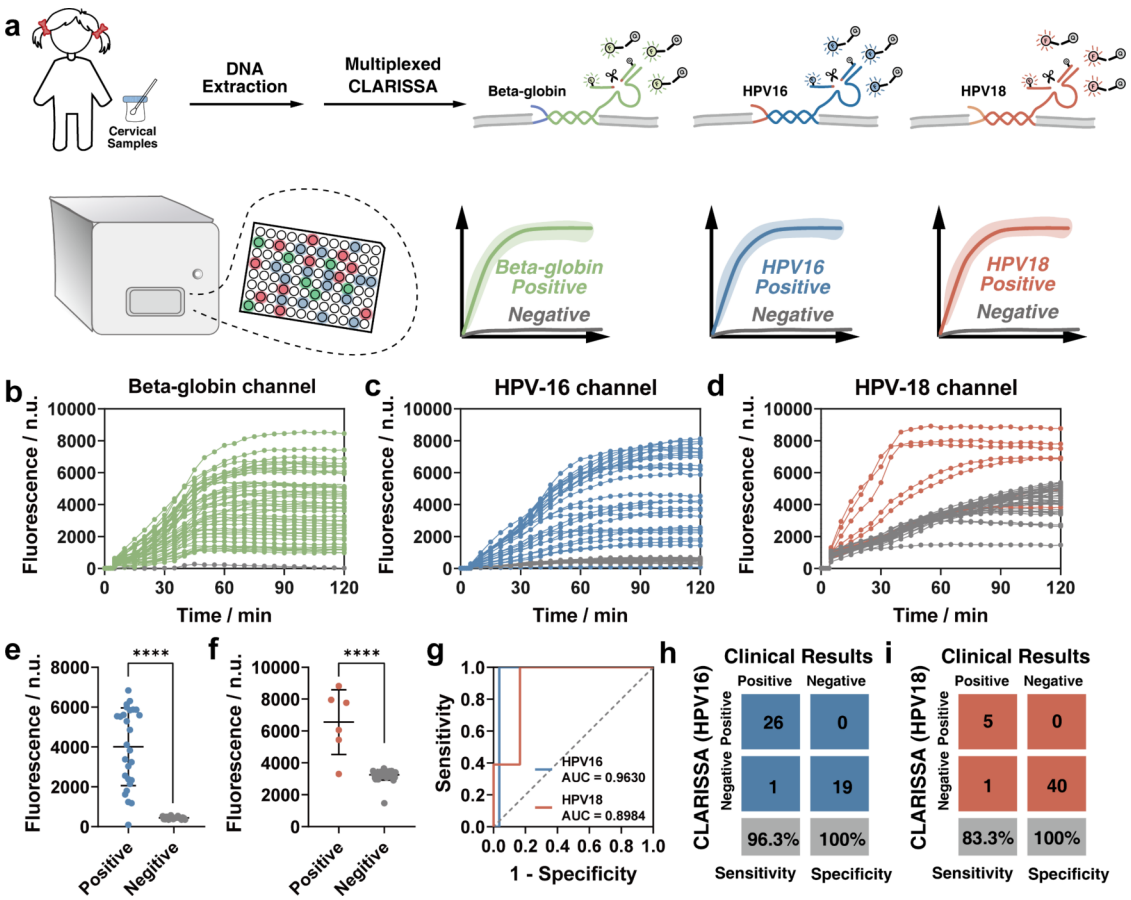

Figure 6. Multiplex CLARISSA. (a) The workflow of the 3-plex CLARISSA for the simultaneous detection of *β*-globin, HPV16, and HPV18 genes in clinical cervical samples. (b–d) Kinetic curves for analyzing *β*-globin (b), HPV16 (c), and HPV18 (d) in 46 clinical cervical samples using the 3-plex CLARISSA. (e) Test results of two clinical cohorts included 27 HPV16 positives and 19 HPV16 negatives. (f) Test results of two clinical cohorts were available, including 6 HPV18 positives and 40 HPV18 negatives. Unpaired two-tailed *t*-tests were used to evaluate statistical differences between clinical cohorts. (g) ROC curves of CLARISSA for 3-plex detection of HPV16 and HPV 18 in 46 human cervical samples. Optimal cutoff fluorescence values were selected through ROC analysis: 873 n.u. at 60 min for HPV16 (specificity = 96.3%; sensitivity = 100%) and 4552 n.u. at 60 min for HPV18 (specificity = 83.3%; sensitivity = 100%). (h, i) Evaluation of the clinical sensitivity and specificity of the 3-plex CLARISSA for HPV16 (h) and HPV18 (i) was done by comparing to clinical screening results using a confusion matrix.

compatible with CLARISSA. We will also integrate CLARISSA with sample preparation units, such as HUDSON,[42] and smartphone-based signal readout unit to enable a sample-in answer-out NAT platform for clinical testing in the field and in POC settings.[43]

■ ASSOCIATED CONTENT

Supporting Information

The Supporting Information is available free of charge at https://pubs.acs.org/doi/10.1021/jacsau.4c00232.

Details of materials and experimental procedures; optimization of cleavage conditions for Dzs and gDzs, characterization of the orthogonality of Dzs and gDzs, Michaelis–Menten analyses of Dzs and gDzs, thermodynamics analyses of gDzs, PAGE analyses of RPA primer screening, clinical validation of CLARISSA with LFA visual readout, characterization of multiplexed CLARISSA (Figures S1–S35), and summarizing DNA sequences and modifications, and clinicopathological characteristics for CLARISSA (Tables S1–S5) (PDF)

■ AUTHOR INFORMATION

Corresponding Author

Feng Li − *Key Laboratory of Green Chemistry & Technology of Ministry of Education, College of Chemistry, Sichuan University, Chengdu, Sichuan 610064, China; Department of Chemistry, Centre for Biotechnology, Brock University, St. Catharines, Ontario L2S 3A1, Canada; Department of Laboratory Medicine, Med+X Center for Manufacturing, West China Hospital, Sichuan University, Chengdu, Sichuan 610041, China;* orcid.org/0000-0002-2616-5343; Email: windtalker_1205@scu.edu.cn

Authors

Lu Gao − *Key Laboratory of Green Chemistry & Technology of Ministry of Education, College of Chemistry, Sichuan University, Chengdu, Sichuan 610064, China*

Ke Yi − *Department of Gynecology and Obstetrics, Key Laboratory of Obstetrics and Gynecologic and Pediatric Diseases and Birth Defects of Ministry of Education, West China Second Hospital, Sichuan University, Chengdu, Sichuan 610041, China*

https://doi.org/10.1021/jacsau.4c00232
JACS Au 2024, 4, 1664–1672

Yun Tan − *Key Laboratory of Green Chemistry & Technology of Ministry of Education, College of Chemistry, Sichuan University, Chengdu, Sichuan 610064, China*
Chen Guo − *Key Laboratory of Green Chemistry & Technology of Ministry of Education, College of Chemistry, Sichuan University, Chengdu, Sichuan 610064, China*
Danxi Zheng − *Department of Gynecology and Obstetrics, Key Laboratory of Obstetrics and Gynecologic and Pediatric Diseases and Birth Defects of Ministry of Education, West China Second Hospital, Sichuan University, Chengdu, Sichuan 610041, China*
Chenlan Shen − *Department of Laboratory Medicine, Med+X Center for Manufacturing, West China Hospital, Sichuan University, Chengdu, Sichuan 610041, China*

Complete contact information is available at: https://pubs.acs.org/10.1021/jacsau.4c00232

Author Contributions

⊥L.G. and K.Y. contributed equally to this work. F.L. conceived the idea, designed all experiments, supervised the overall project, analyzed the data, and wrote the paper. L.G. and K.Y. designed CLARISSA assay and all characterization experiments. L.G., K.Y., C.G., and D.Z. collected all clinical cervical samples from cervical screening. L.G. and C.G. performed all sample preparation for clinical samples and extracted gDNA. L.G. and Y.T. performed CLARISSA integrated with lateral flow reaction. All authors participated in the drafting and revision of the manuscript.

Notes

The authors declare the following competing financial interest(s): There is a pending patent for CLARISSA technology.

■ ACKNOWLEDGMENTS

We thank the Science and Technology Major Project of the Tibetan Autonomous Region of China (XZ202201ZD0001G), the National Natural Science Foundation of China (22074099), and the Institutional Research Fund from Sichuan University (2021SCUNL105) for financial support.

■ REFERENCES

(1) Urdea, M.; Penny, L. A.; Olmsted, S. S.; Giovanni, M. Y.; Kaspar, P.; Shepherd, A.; Wilson, P.; Dahl, C. A.; Buchsbaum, S.; Moeller, G.; Hay Burgess, D. C. Requirements for high impact diagnostics in the developing world. *Nature* **2006**, *444*, 73−79.
(2) Wu, L.; Qu, X. Cancer biomarker detection: recent achievements and challenges. *Chem. Soc. Rev.* **2015**, *44*, 2963−2997.
(3) Broza, Y. Y.; Zhou, X.; Yuan, M. M.; Qu, D. Y.; Zheng, Y. B.; Vishinkin, R.; Khatib, M.; Wu, W. W.; Haick, H. Disease Detection with Molecular Biomarkers: From Chemistry of Body Fluids to Nature-Inspired Chemical Sensors. *Chem. Rev.* **2019**, *119*, 11761−11817.
(4) Crosby, D.; Bhatia, S.; Brindle, K. M.; Coussens, L. M.; Dive, C.; Emberton, M.; Esener, S.; Fitzgerald, R. C.; Gambhir, S. S.; Kuhn, P.; Rebbeck, T. R.; Balasubramanian, S. Early detection of cancer. *Science* **2022**, *375*, No. eaay9040.
(5) Li, M.; Yin, F.; Song, L.; Mao, X.; Li, F.; Fan, C.; Zuo, X.; Xia, Q. Nucleic Acid Tests for Clinical Translation. *Chem. Rev.* **2021**, *121*, 10469−10558.
(6) Zhao, Y. X.; Zuo, X. L.; Li, Q.; Chen, F.; Chen, Y. R.; Deng, J. Q.; Han, D.; Hao, C. L.; Huang, F. J.; Huang, Y. Y.; Ke, G. L.; Kuang, H.; Li, F.; Li, J.; Li, M.; Li, N.; Lin, Z. Y.; Liu, D. B.; Liu, J. W.; Liu, L. B.; Liu, X. G.; Lu, C. H.; Luo, F.; Mao, X. H.; Sun, J. S.; Tang, B.; Wang, F.; Wang, J. B.; Wang, L. H.; Wang, S.; Wu, L. L.; Wu, Z. S.; Xia, F.; Xu, C. L.; Yang, Y.; Yuan, B. F.; Yuan, Q.; Zhang, C.; Zhu, Z.; Yang, C. Y.; Zhang, X. B.; Yang, H. H.; Tan, W. H.; Fan, C. H. Nucleic Acids Analysis. *Sci. China Chem.* **2021**, *64*, 171−203.
(7) Shen, M. Z.; Zhou, Y.; Ye, J. W.; Al-Maskri, A. A. A.; Kang, Y.; Zeng, S.; Cai, S. Recent advances and perspectives of nucleic acid detection for coronavirus. *J. Pharm. Anal.* **2020**, *10*, 97−101.
(8) Yang, S.; Rothman, R. E. PCR-based diagnostics for infectious diseases: uses, limitations, and future applications in acute-care settings. *Lancet Infect. Dis.* **2004**, *4*, 337−348.
(9) Gubala, V.; Harris, L. F.; Ricco, A. J.; Tan, M. X.; Williams, D. E. Point of Care Diagnostics: Status and Future. *Anal. Chem.* **2012**, *84*, 487−515.
(10) Wang, C.; Liu, M.; Wang, Z. F.; Li, S.; Deng, Y.; He, N. Y. Point-of-care diagnostics for infectious diseases: From methods to devices. *Nano Today* **2021**, *37*, No. 101092, DOI: 10.1016/j.nantod.2021.101092.
(11) Zhang, Z. W.; Ma, P.; Ahmed, R.; Wang, J.; Akin, D.; Soto, F.; Liu, B. F.; Li, P. W.; Demirci, U. Advanced Point-of-Care Testing Technologies for Human Acute Respiratory Virus Detection. *Adv. Mater.* **2022**, *34*, No. 2103646, DOI: 10.1002/adma.202103646.
(12) Vashist, S. K.; Luppa, P. B.; Yeo, L. Y.; Ozcan, A.; Luong, J. H. T. Emerging Technologies for Next-Generation Point-of-Care Testing. *Trends Biotechnol.* **2015**, *33*, 692−705.
(13) Kaminski, M. M.; Abudayyeh, O. O.; Gootenberg, J. S.; Zhang, F.; Collins, J. J. CRISPR-based diagnostics. *Nat. Biomed. Eng.* **2021**, *5*, 643−656.
(14) Abudayyeh, O. O.; Gootenberg, J. S. CRISPR diagnostics. *Science* **2021**, *372*, 914−915.
(15) Tang, Y.; Gao, L.; Feng, W.; Guo, C.; Yang, Q.; Li, F.; Le, X. C. The CRISPR−Cas toolbox for analytical and diagnostic assay development. *Chem. Soc. Rev.* **2021**, *50*, 11844−11869.
(16) Li, H.; Xie, Y.; Chen, F.; Bai, H.; Xiu, L.; Zhou, X.; Guo, X.; Hu, Q.; Yin, K. Amplification-free CRISPR/Cas detection technology: challenges, strategies, and perspectives. *Chem. Soc. Rev.* **2023**, *52*, 361−382.
(17) Li, Y.; Li, S. Y.; Wang, J.; Liu, G. CRISPR/Cas Systems towards Next-Generation Biosensing. *Trends Biotechnol.* **2019**, *37*, 730−743.
(18) Han, J.; Shin, J.; Lee, E. S.; Cha, B. S.; Kim, S.; Jang, Y.; Kim, S.; Park, K. S. Cas12a/blocker DNA-based multiplex nucleic acid detection system for diagnosis of high-risk human papillomavirus infection. *Biosens. Bioelectron.* **2023**, *232*, No. 115323.
(19) Yoon, T.; Shin, J.; Choi, H.-J.; Park, K. S. Split T7 promoter-based isothermal transcription amplification for one-step fluorescence detection of SARS-CoV-2 and emerging variants. *Biosens. Bioelectron.* **2022**, *208*, No. 114221.
(20) Shin, J.; Yoon, T.; Nam, D.; Kim, D.; Kim, S.; Cha, B. S.; Lee, E. S.; Jang, Y.; Kim, S.; Han, J.; Choi, H.-J.; Park, K. S. Multipurpose advanced split T7 promoter-based transcription amplification for ultrasensitive molecular diagnostics. *Chem. Eng. J.* **2023**, *464*, No. 142614.
(21) Lyu, M.; Kong, L.; Yang, Z.; Wu, Y.; McGhee, C. E.; Lu, Y. PNA-Assisted DNAzymes to Cleave Double-Stranded DNA for Genetic Engineering with High Sequence Fidelity. *J. Am. Chem. Soc.* **2021**, *143*, 9724−9728.
(22) Gu, J.; Mathai, A.; Nurmi, C.; White, D.; Panesar, G.; Yamamura, D.; Balion, C.; Gubbay, J.; Mossman, K.; Capretta, A.; Salena, B. J.; Soleymani, L.; Filipe, C. D. M.; Brennan, J. D.; Li, Y. Detection of Large Genomic RNA via DNAzyme-Mediated RNA Cleavage and Rolling Circle Amplification: SARS-CoV-2 as a Model. *Chem. - Eur. J.* **2023**, *29*, No. e202300075.
(23) Shi, C.; Yang, D.; Ma, X.; Pan, L.; Shao, Y.; Arya, G.; Ke, Y.; Zhang, C.; Wang, F.; Zuo, X.; Li, M.; Wang, P. A Programmable DNAzyme for the Sensitive Detection of Nucleic Acids. *Angew. Chem., Int. Ed.* **2024**, *63*, No. e202320179.
(24) Safdar, S.; Lammertyn, J.; Spasic, D. RNA-Cleaving NAzymes: The Next Big Thing in Biosensing? *Trends Biotechnol.* **2020**, *38*, 1343−1359.
(25) Mokany, E.; Bone, S. M.; Young, P. E.; Doan, T. B.; Todd, A. V. MNAzymes, a versatile new class of nucleic acid enzymes that can

function as biosensors and molecular switches. *J. Am. Chem. Soc.* **2010**, *132*, 1051−1059.
(26) Zagorovsky, K.; Chan, W. C. W. A Plasmonic DNAzyme Strategy for Point-of-Care Genetic Detection of Infectious Pathogens. *Angew. Chem., Int. Ed.* **2013**, *52*, 3168−3171.
(27) Mohamed, M. A. A.; Kozlowski, H. N.; Kim, J.; Zagorovsky, K.; Kantor, M.; Feld, J. J.; Mubareka, S.; Mazzulli, T.; Chan, W. C. W. Diagnosing Antibiotic Resistance Using Nucleic Acid Enzymes and Gold Nanoparticles. *ACS Nano* **2021**, *15*, 9379−9390.
(28) Yang, K.; Chaput, J. C. REVEALR: A Multicomponent XNAzyme-Based Nucleic Acid Detection System for SARS-CoV-2. *J. Am. Chem. Soc.* **2021**, *143*, 8957−8961.
(29) Yang, K.; Schuder, D. N.; Ngor, A. K.; Chaput, J. C. REVEALR-Based Genotyping of SARS-CoV-2 Variants of Concern in Clinical Samples. *J. Am. Chem. Soc.* **2022**, *144*, 11685−11692.
(30) Yang, K.; Chaput, J. C. Amplification-Free COVID-19 Detection by Digital Droplet REVEALR. *ACS Synth. Biol.* **2023**, *12*, 1331−1338.
(31) Santoro, S. W.; Joyce, G. F. A general purpose RNA-cleaving DNA enzyme. *Proc. Natl. Acad. Sci. U.S.A.* **1997**, *94*, 4262−4266.
(32) Cairns, M. J.; King, A.; Sun, L. Q. Optimisation of the 10−23 DNAzyme−substrate pairing interactions enhanced RNA cleavage activity at purine−cytosine target sites. *Nucleic Acids Res.* **2003**, *31*, 2883−2889.
(33) Woodman, C. B. J.; Collins, S. I.; Young, L. S. The natural history of cervical HPV infection: unresolved issues. *Nat. Rev. Cancer* **2007**, *7*, 11−22.
(34) Burk, R. D.; Chen, Z. G.; Saller, C.; Tarvin, K.; Carvalho, A. L.; Scapulatempo-Neto, C.; Silveira, H. C.; Fregnani, J. H.; Creighton, C. J.; Anderson, M. L.; Castro, P.; Wang, S. S.; Yau, C.; Benz, C.; Robertson, A. G.; Mungall, K.; Lim, L.; Bowlby, R.; Sadeghi, S.; Brooks, D.; Sipahimalani, P.; Mar, R.; Ally, A.; Clarke, A.; Mungall, A. J.; Tam, A.; Lee, D.; Chuah, E.; Schein, J. E.; Tse, K.; Kasaian, K.; Ma, Y.; Marra, M. A.; Mayo, M.; Balasundaram, M.; Thiessen, N.; Dhalla, N.; Carlsen, R.; Moore, R. A.; Holt, R. A.; Jones, S. J. M.; Wong, T. N.; Pantazi, A.; Parfenov, M.; Kucherlapati, R.; Hadjipanayis, A.; Seidman, J.; Kucherlapati, M.; Ren, X. J.; Xu, A. W.; Yang, L. X.; Park, P. J.; Lee, S.; Rabeno, B.; Huelsenbeck-Dill, L.; Borowsky, M.; Cadungog, M.; Iacocca, M.; Petrelli, N.; Swanson, P.; Ojesina, A. I.; Le, X.; Sandusky, G.; Adebamowo, S. N.; Akeredolu, T.; Adebamowo, C.; Reynolds, S. M.; Shmulevich, I.; Shelton, C.; Crain, D.; Mallery, D.; Curley, E.; Gardner, J.; Penny, R.; Morris, S.; Shelton, T.; Liu, J.; Lolla, L.; Chudamani, S.; Wu, Y.; Birrer, M.; McLellan, M. D.; Bailey, M. H.; Miller, C. A.; Wyczalkowski, M. A.; Fulton, R. S.; Fronick, C. C.; Lu, C.; Mardis, E. R.; Appelbaum, E. L.; Schmidt, H. K.; Fulton, L. A.; Cordes, M. G.; Li, T. D.; Ding, L.; Wilson, R. K.; Rader, J. S.; Behmaram, B.; Uyar, D.; Bradley, W.; Wrangle, J.; Pastore, A.; Levine, D. A.; Dao, F.; Gao, J. J.; Schultz, N.; Sander, C.; Ladanyi, M.; Einstein, M.; Teeter, R.; Benz, S.; Wentzensen, N.; Felau, I.; Zenklusen, J. C.; Bodelon, C.; Demchok, J. A.; Yang, L. M.; Sheth, M.; Ferguson, M. L.; Tarnuzzer, R.; Yang, H. N.; Schiffman, M.; Zhang, J. S.; Wang, Z. N.; Davidsen, T.; Olaniyan, O.; Hutter, C. M.; Sofia, H. J.; Gordenin, D. A.; Chan, K.; Roberts, S. A.; Klimczak, L. J.; Van Waes, C.; Chen, Z.; Saleh, A. D.; Cheng, H.; Parfitt, J.; Bartlett, J.; Albert, M.; Arnaout, A.; Sekhon, H.; Gilbert, S.; Peto, M.; Myers, J.; Harr, J.; Eckman, J.; Bergsten, J.; Tucker, K.; Zach, L. A.; Karlan, B. Y.; Lester, J.; Orsulic, S.; Sun, Q. Integrated genomic and molecular characterization of cervical cancer. *Nature* **2017**, *543*, 378−384.
(35) Ramachandran, A.; Santiago, J. G. CRISPR Enzyme Kinetics for Molecular Diagnostics. *Anal. Chem.* **2021**, *93*, 7456−7464.
(36) Huyke, D. A.; Ramachandran, A.; Bashkirov, V. I.; Kotseroglou, E. K.; Kotseroglou, T.; Santiago, J. G. Enzyme Kinetics and Detector Sensitivity Determine Limits of Detection of Amplification-Free CRISPR-Cas12 and CRISPR-Cas13 Diagnostics. *Anal. Chem.* **2022**, *94*, 9826−9834.
(37) Nalefski, E. A.; Patel, N.; Leung, P. J. Y.; Islam, Z.; Kooistra, R. M.; Parikh, I.; Marion, E.; Knott, G. J.; Doudna, J. A.; Le Ny, A.-L. M.; Madan, D. Kinetic analysis of Cas12a and Cas13a RNA-Guided nucleases for development of improved CRISPR-Based diagnostics. *iScience* **2021**, *24*, No. 102996.
(38) Piepenburg, O.; Williams, C. H.; Stemple, D. L.; Armes, N. A. DNA detection using recombination proteins. *PLoS Biol.* **2006**, *4*, No. e204.
(39) Wang, G. A.; Xie, X.; Mansour, H.; Chen, F.; Matamoros, G.; Sanchez, A. L.; Fan, C.; Li, F. Expanding detection windows for discriminating single nucleotide variants using rationally designed DNA equalizer probes. *Nat. Commun.* **2020**, *11*, No. 5473.
(40) Schiffman, M.; Castle, P. E.; Jeronimo, J.; Rodriguez, A. C.; Wacholder, S. Human papillomavirus and cervical cancer. *Lancet* **2007**, *370*, 890−907.
(41) Crosbie, E. J.; Einstein, M. H.; Franceschi, S.; Kitchener, H. C. Human papillomavirus and cervical cancer. *Lancet* **2013**, *382*, 889−899.
(42) Myhrvold, C.; Freije, C. A.; Gootenberg, J. S.; Abudayyeh, O. O.; Metsky, H. C.; Durbin, A. F.; Kellner, M. J.; Tan, A. L.; Paul, L. M.; Parham, L. A.; Garcia, K. F.; Barnes, K. G.; Chak, B.; Mondini, A.; Nogueira, M. L.; Isern, S.; Michael, S. F.; Lorenzana, I.; Yozwiak, N. L.; MacInnis, B. L.; Bosch, I.; Gehrke, L.; Zhang, F.; Sabeti, P. C. Field-deployable viral diagnostics using CRISPR-Cas13. *Science* **2018**, *360*, 444−448.
(43) Arizti-Sanz, J.; Bradley, A. D.; Zhang, Y. B.; Boehm, C. K.; Freije, C. A.; Grunberg, M. E.; Kosoko-Thoroddsen, T.-S. F.; Welch, N. L.; Pillai, P. P.; Mantena, S.; Kim, G.; Uwanibe, J. N.; John, O. G.; Eromon, P. E.; Kocher, G.; Gross, R.; Lee, J. S.; Hensley, L. E.; MacInnis, B. L.; Johnson, J.; Springer, M.; Happi, C. T.; Sabeti, P. C.; Myhrvold, C. Simplified Cas13-based assays for the fast identification of SARS-CoV-2 and its variants. *Nat. Biomed. Eng.* **2022**, *6*, 932−943.

https://doi.org/10.1021/jacsau.4c00232
JACS Au 2024, 4, 1664−1672